Lyle, M., Koizumi, I., Richter, C., and Moore, T.C., Jr. (Eds.), 2000
Proceedings of the Ocean Drilling Program, Scientific Results, Vol. 167

12. LATE QUATERNARY RECORDS OF ORGANIC CARBON, CALCIUM CARBONATE, AND BIOMARKERS FROM SITE 1016 OFF POINT CONCEPTION, CALIFORNIA MARGIN[1]

Masanobu Yamamoto,[2] Masumi Yamamuro,[3] and Ryuji Tada[4]

ABSTRACT

Total organic carbon (TOC) and calcium carbonate ($CaCO_3$) concentrations were determined for 304 samples, and biomarkers were analyzed for 101 samples from Core 167-1016C-1H. TOC varies between 1% and 2%, and $CaCO_3$ is typically 1%–4%, with peaks reaching 14%.

Paleotemperature estimated from $U^{k'}_{37}$ varies from 8.5° to 17.5°C. The $U^{k'}_{37}$ variation implies that Core 167-1016C-1H covers oxygen isotope Stages 1–6.

Peaks of diatom-derived $C_{25:1}$ HBI alkene concentrations occur during warming intervals, suggesting intensified upwelling during deglaciation. The concentrations of haptophyte-derived alkenones and diatom-derived $C_{25:1}$ HBI alkene vary out of phase, which presumably resulted from the changes in the mode of nutrient supply to surface mixed layer.

Maximal $CaCO_3$ contents (>10%) were observed in both warming and cooling intervals. The peak in cooling interval relates to an alkenone maximum, whereas the peaks in warming intervals do not. This implies that carbonate production is not the only factor controlling carbonate compensation depth at this site, and it suggests considering the changes in North Pacific deep-water chemistry.

Petroleum-type compounds are present in Site 1016 sediments. Their concentrations are maximized in the warming intervals that correspond to the timing of destruction of a huge tar mound off Point Conception. The tarry material was presumably transported by the Arguello Fan system to Site 1016.

INTRODUCTION

Ocean Drilling Program (ODP) Site 1016 (34°32′N, 122°17′W) is located about 150 km west of Point Conception, California, on an abyssal hill in water 3835 m deep (Fig. 1). Although the Monterey Fan and the Arguello Fan extend to the north and south, respectively, of this abyssal hill (Chase et al., 1981), this site is covered with hemipelagic sediments. The core of southward flow of the California Current is located near this site (Hickey, 1979; Lynn and Simpson, 1987). The site is, therefore, suitable for reconstructing sea-surface temperature (SST) of the California Current and the intensity of its associated upwelling. The SST of the California Current is the result of mixing the West Wind Drift subarctic water and the North Pacific Current subtropical water (Hickey, 1979), and it is possibly sensitive to climate changes in the North Pacific Ocean and the surrounding areas. The coastal upwelling is induced by northerly winds along the California margin (Huyer, 1983), and the changes in its intensity affect primary productivity and the ecosystem (e.g., Parsons et al., 1984; Roemmich and McGown, 1995). Thus the assessments of paleo-sea-surface temperature (paleo-SST), primary productivity, and the marine ecosystem provide a clue to understanding the responses of the California Current system to Quaternary climate changes.

Many investigations have been conducted on the paleoenvironmental changes along the California margin, and most of them focused on the changes during the last 30,000 yr. ODP Site 893 provided 197-m-long core of sediments from the Santa Barbara Basin for high-resolution late Quaternary paleoenvironmental studies (Shore-based Scientific Party, 1994). During Leg 167, we drilled Sites 1016 (3846 m water depth) and 1017 (967 m water depth) at the open-

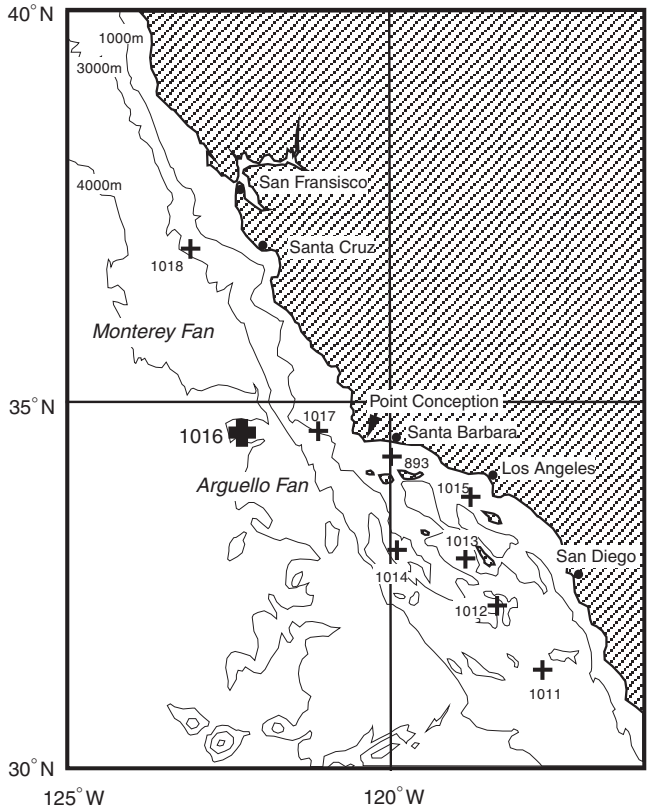

Figure 1. Location of Site 1016 off Point Conception.

[1]Lyle, M., Koizumi, I., Richter, C., and Moore, T.C., Jr. (Eds.), 2000. *Proc. ODP, Sci. Results,* 167: College Station TX (Ocean Drilling Program).

[2]Mineral and Fuel Resources Department, Geological Survey of Japan, 1-1-3 Higashi, Tsukuba, Ibaraki 305-8567, Japan. yamamoto@gsj.go.jp

[3]Marine Geology Department, Geological Survey of Japan, 1-1-3 Higashi, Tsukuba, Ibaraki 305-8567, Japan.

[4]Geological Institute, University of Tokyo, 7-3-1 Hongo, Bunkyo-ku, Tokyo 113, Japan.

ocean side of the Santa Barbara Basin. The location of Site 1016 is a hemipelagic, deep-sea site; therefore, the sediments record sensitively the changes of marine surface environment and carbonate compensation depth.

Assessments of paleo-SST were conducted using proxies of alkenones, foraminifers, radiolarians, and pollens during the last 30,000 yr at many locations along the California margin and during the last 160,000 yr at Site 893. Along the northern California margin, the paleo-SST estimated using $U^{k'}_{37}$ (Prahl et al., 1995; Doose et al., 1997) agrees with those estimated using radiolarian assemblages (Prahl et al., 1995) and foraminiferal $\delta^{18}O$ and their assemblages (Ortiz et al., 1997), and both indicate about 4°C lower SST in the last glacial maximum (LGM; Stage 2) than the Holocene (Stage 1). In contrast, in the California Borderland, $U^{k'}_{37}$-derived SST disagrees with foraminiferal and pollen-derived SST during LGM. The $U^{k'}_{37}$-SST estimates indicate that LGM was 0°–2°C cooler than Holocene (Herbert et al., 1995; Hinrichs et al., 1997), whereas the SST estimations using sinistral/dextral ratio of *N. pachyderma*, $\delta^{18}O$ of planktonic foraminifers, and foraminiferal assemblages indicate that LGM was more than 5°C cooler than Holocene (Kahn et al., 1981; Kennett and Ingram, 1995; Kennett and Venz, 1995; Thunell and Mortyn, 1995; Mortyn et al., 1996). Pollen assemblages at Site 893 agreed with foraminiferal SST estimation (Heusser, 1995).

Primary productivity changes along the California margin were assessed based on the contents and accumulation rates of organic carbon, calcium carbonate, trace elements, and opaline skeletons. Along the northern California margin, changes in the organic carbon and diatom accumulation rates and trace metal concentrations suggest that the productivity during LGM was lower than Holocene (Lyle et al., 1992; Sancetta et al., 1992; Ortiz et al., 1997; Dean et al., 1997; Gardner et al., 1997), which was attributed to weaker coastal-upwelling–favorable northerly winds off northern California and Oregon during LGM (Lyle et al., 1992; Sancetta et al., 1992). The weaker upwelling during LGM was also indicated by Doose et al. (1997), who suggested the decreased intensity of the California Current during LGM, based on the increased SST gradient along the California margin. In the California Borderland, lower productivity during LGM than Holocene was suggested in the Santa Barbara Basin (Berger et al., 1997), whereas higher productivity was suggested in several other basins (Mortyn and Thunell, 1997). Mortyn and Thunell (1997) suggested that southerly migration of the North Pacific High resulted in upwelling intensification and increased productivity during LGM. In the Santa Barbara Basin, the studies of cores from Site 893 demonstrated the higher organic accumulation rates at Substages 5a, 5c, and 5e (Gardner and Dartnell, 1995: Stein and Rack, 1995), which was attributed to higher productivity at these periods (Stein and Rack, 1995).

The changes of carbonate compensation depth (CCD) in the last 300,000-yr were examined in the range 2700–4300 m deep along the northern California and Oregon margins, and it was suggested that the CCD has migrated more than 1800 m between glacial and interglacial times (Karlin et al., 1992). This large carbonate fluctuation was attributed to regional mechanisms, such as the glacial deep-water formation in the northern Pacific Ocean or the enhanced dissolution due to interglacial noncarbonate productivity related to coastal upwelling (Karlin et al., 1992). On the other hand, Gardner et al. (1997) found a carbonate preservation event at 10 ka in cores from the northern California margin and attributed it to the global mechanism, hypothesized by Broecker et al. (1993), that the expansion of boreal forests in the northern hemisphere removed CO_2 from the atmosphere and the surface water of the ocean, and in turn increased alkalinity of ocean water, which should have resulted in greater preservation of calcium carbonate.

The origin of organic matter in California and Oregon margin sediments was investigated in detail using various organic geochemical indicators including C/N value and Rock-Eval parameters (e.g., Rullkötter et al., 1981; Stein and Rack, 1995), lignin concentration (e.g., Hedges and Mann, 1979), and biomarker concentrations (e.g., Simoneit, 1977; Simoneit and Kaplan, 1980; Venkatesan et al., 1980; McEvoy et al., 1981; Louda and Baker, 1981; Simoneit and Mazurek, 1981; Rullkötter et al., 1981; Prahl and Carpenter, 1984; Venkatesan et al., 1990; Kennedy and Brassell, 1992; Hinrichs et al., 1995). Sediment trap samples were also examined for the biomarkers associated with sinking particles in the California Borderland (e.g., Crisp et al., 1979; Venkatesan and Kaplan, 1992). These studies indicate the contributions of marine algae, bacteria, and higher plants to the organic matter in California and Oregon margin sediments. In addition, petroleum-type components were characteristically observed in recent sediments (Simoneit and Kaplan, 1980; Venkatesan et al., 1980), late Pleistocene sediments (Hinrichs et al., 1995), and sinking particles (Crisp et al., 1979; Venkatesan and Kaplan, 1992) from the California Borderland, and their source was hypothesized to be anthropogenic pollution, submarine seep oils, and weathered matured petroleum source rocks.

In this preliminary study, we examine the changes of organic carbon and calcium carbonate contents, alkenone unsaturation indices, and biomarker concentrations in Core 167-1016C-1H, and discuss the responses of the marine ecosystem to climate changes during the late Quaternary, carbonate dissolution changes, and the origin of petroleum-type components in the sediments.

SAMPLES AND METHODS

Samples

The sediments of Core 167-1016C-1H (0–9.2 mbsf) consist of gradationally interbedded dark gray to dark greenish gray diatom ooze with clay, grayish olive diatom clay, clayey diatom ooze, and light greenish yellow to light olive gray diatom nannofossil ooze with clay. Smear-slide observation indicates that diatom frustules compose 36%–60% of the sediments (Shipboard Scientific Party, 1997a). Our observation using soft X-ray radiographs reveals that burrows occur throughout the whole range of this core, indicating constantly oxic depositional environment (Fig. 2).

Core 167-1016C-1H was sealed in a N_2-filled oxygen-impermeable plastic bag immediately after the recovery and stored in a refrigerator for three months until shore-based sampling. Samples of ~20 cm^3 in volume were taken every 3 cm and immediately frozen in N_2-filled Kapack bags.

Analytical Method

Three hundred-four freeze-dried sediment samples at 3-cm intervals were analyzed for total organic carbon (TOC), total carbon (TC), and total nitrogen (TN) using a Yanaco MT-5 elemental analyzer. To remove carbonate carbon, the samples were acidified following the method of Yamamuro and Kayanne (1995). Inorganic carbon (IC) and calcium carbonate ($CaCO_3$) contents were calculated according to the following equations:

$$IC = TC - TOC, \text{ and}$$

$$CaCO_3 = IC \times 8.333.$$

One hundred and one freeze-dried sediment samples (1 g) taken at 9-cm intervals were extracted by ultrasonification with 10 mL of dichloromethane/methanol (6/4 v/v) for 5 min three times. The lipid extract was separated into five fractions (F1: 3 mL of hexane; F2: 3 mL of hexane/toluene (3/1 v/v); F3: 4 mL of toluene; F4: 3 mL of toluene/methanol (3/1 v/v); and F5: 3 mL of methanol) by column chromatography (SiO_2 with 5% distilled water, i.d. 5.5 mm, 45 mm long). *n*-$C_{24}D_{50}$ and *n*-$C_{36}H_{74}$ were added as internal standards into the F1 and F3 fractions, respectively.

Gas chromatography was conducted using a Hewlett Packard 5890 series II gas chromatograph (GC) with on-column injection and

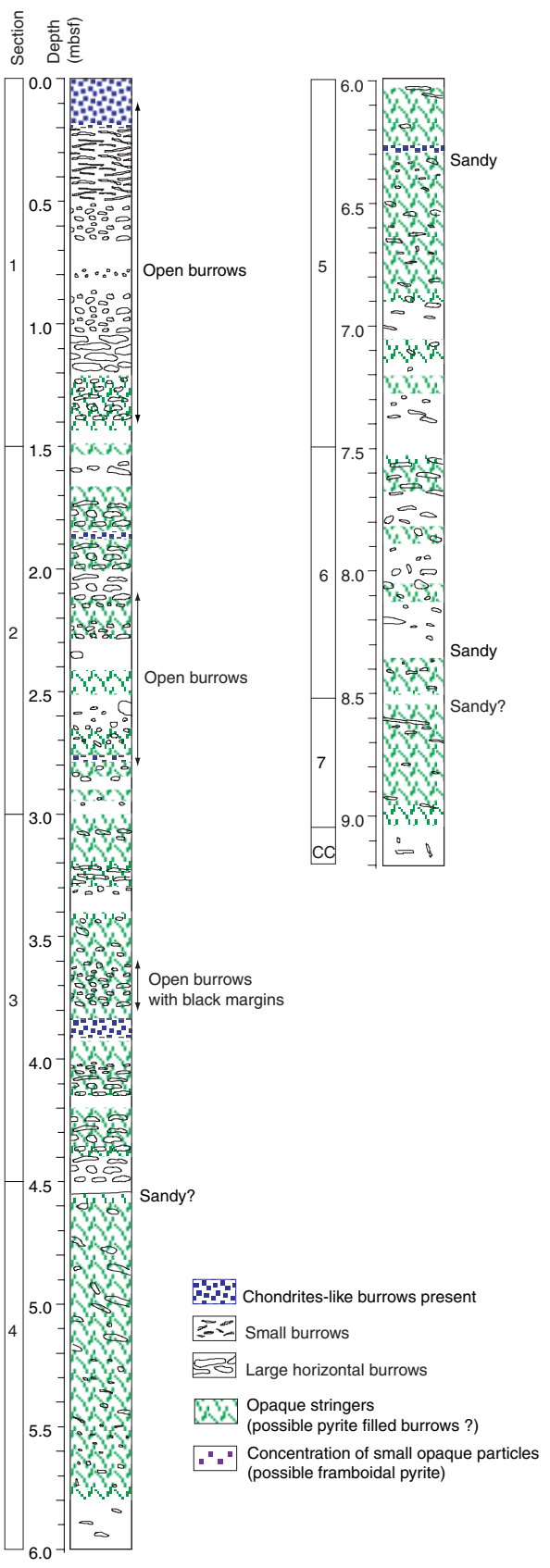

Figure 2. Core 167-1016C-1H columnar section based on visual observation and soft X-ray radiograph.

electronic pressure control systems and a flame ionization detector. The F1 (hydrocarbon) fraction was analyzed using a capillary column coated with Chrompack CP-Sil5CB (30 m long, i.d. 0.25 mm, 0.25 µm thick). The oven temperature was programmed from 70° to 130°C at 20°C/min, from 130° to 310°C at 4°C/min., and then held at 310°C for 15 min. The F3 (alkenone) fraction was analyzed using a capillary column coated with Chrompack CP-Sil5CB (60 m, i.d. 0.25 mm, 0.25 µm thick). The oven temperature was programmed from 70° to 310°C at 20°C/min and then held at 310°C for 60 min. Helium was used as a carrier gas, and the flow velocity was maintained at 30 cm/s.

Gas chromatography-mass spectrometry was conducted using a Hewlett Packard 5973 gas chromatograph-mass selective detector with on-column injection and electronic pressure control systems and quadrupole mass spectrometer. The GC column for F3 analysis and oven temperature and carrier pressure programs are the same as above. For F1 analysis, 60-m-long CP-Sil5CB (i.d. 0.25 mm, 0.25 µm thick) was used instead of 30-m-long column. The mass spectrometer was run in the full scan ion monitoring mode (*m/z* 50–650). Electron impact spectra were obtained at 70 eV. Identification of compounds was achieved by comparison of their mass spectra and retention times with those in the literature.

The alkenone unsaturation index $U^{k'}_{37}$ was calculated from the concentrations of di- and tri-unsaturated C_{37} alken-2-ones (C_{37}MK) using the expression (Brassell et al., 1986)

$$U^{k'}_{37} = [C_{37:2}MK]/([C_{37:2}MK] + [C_{37:3}MK]).$$

The calculation of temperature was conducted according to the equation: $U^{k'}_{37} = 0.034T + 0.039$ (T = temperature [°C]), based on an experimental result for cultured strain 55a of *Emiliania huxleyi* (Prahl et al., 1988) with an estimated analytical accuracy of 0.5°C (Prahl and Wakeham, 1987). The additional unsaturation indices, U^{me}_{36} and $K_{37:4}/K_{37}$, were calculated using the following equations, respectively (Prahl et al., 1995):

$$U^{me}_{36} = [C_{36:2}ME]/([C_{36:2}ME] + [C_{36:3}ME]),$$

where $[C_{36}ME]$ is the concentration of C_{36} fatty acid-methyl ester, and

$$K_{37:4}/K_{37} = [C_{37:4}MK]/([C_{37:2}MK] + [C_{37:3}MK] + [C_{37:4}MK]).$$

RESULTS

Alkenone Unsaturation Indices

Figure 3 illustrates the variations of alkenone unsaturation indices. Paleotemperature estimated from $U^{k'}_{37}$ varies from 8.5° to 17.5°C. The temperature of the top 54 cm of core ranges between 13.8° and 14.5°C, which agrees with the present mean annual SST at this site (Robinson, 1976). This result is concordant with the recent observation that core-top $U^{k'}_{37}$-derived temperatures represent the mean annual SST along the California margin (Herbert et al., 1998).

The variations of U^{me}_{36} and $K_{37:4}/K_{37}$ are very similar to that of $U^{k'}_{37}$. A good correlation ($r = 0.92$) exists between U^{me}_{36} and $U^{k'}_{37}$. This suggests a single source of $C_{37:2\text{-}4}$ alken-2-one and $C_{37:2\text{-}3}$ methylalkenoates in Core 167-1016C-1H.

The variation of $U^{k'}_{37}$ at Site 1016 is also similar to both $\delta^{18}O$ profiles of planktonic and benthic foraminifers (Kennett et al., Chap. 21, this volume) and $U^{k'}_{37}$ variation (Shipboard Scientific Party, 1997b) at the adjacent shallower Site 1017. Comparison with the oxygen isotope stratigraphy of Site 1017 (Kennett et al., Chap. 21, this volume) enables us to make a preliminary $U^{k'}_{37}$ -based stratigraphy of Site 1016, as shown in Figure 3. This preliminary age-depth model implies that Core 167-1016C-1H covers oxygen isotope Stages 1–6, with the average linear sedimentation rate of 6.4 cm/k.y. The precise age-depth model needs future investigations such as the analyses of

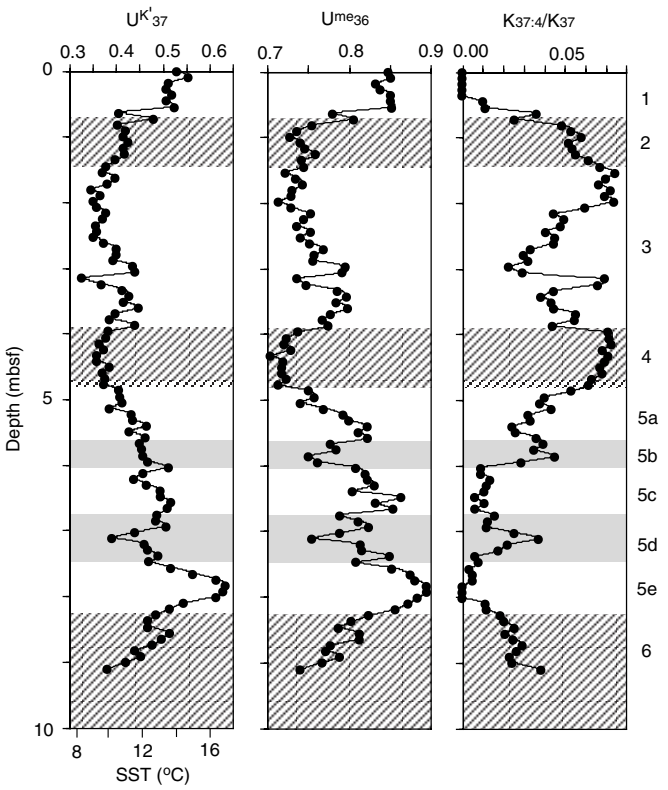

Figure 3. $U^{k'}_{37}$, U^{me}_{36}, and $K_{37:4}/K_{37}$ indices and the sea-surface temperature estimated from $U^{k'}_{37}$ of Core 167-1016C-1H sediments. $U^{k'}_{37}$-based preliminary oxygen-isotope stages are marked with their numbers. Data are listed in Appendix A.

^{14}C of foraminifers, radioactive elements, and amino acid racemization.

Total Organic Carbon, Total Nitrogen, and Calcium Carbonate Contents

Figure 4 illustrates the variations of total organic carbon (TOC), total nitrogen (TN), and calcium carbonate ($CaCO_3$) contents, and the TOC/TN value of Core 167-1016C-1H.

TOC varies between 0.8% and 2.3%, with an average of 1.3%. High TOC contents (>1.5%) occur in the core-top interval (0–0.12 mbsf), at 5.1–6.2 mbsf (Peaks D, E, and F in Fig. 4), 7.3 mbsf (Peak G), and 8.2 mbsf (Peak H). TOC/TN values range between 5.4 and 10.0, with an average of 7.5, indicating predominantly marine origin of the organic matter supplied to this site. $CaCO_3$ content varies between 0% and 13.7%, with an average of 2.5%. Maxima of $CaCO_3$ content (>10%) occur around 0.5 mbsf (Peak I in Fig. 4), 5.2 mbsf (Peak J), and 7.2 mbsf (Peak K). The background value of $CaCO_3$ contents is nearly 0%, which indicates the dissolution of calcium carbonate below the carbonate compensation depth.

Biomarkers

The F1 (hydrocarbon) and F3 (alkenone) fractions were analyzed by gas chromatography and gas chromatography–mass spectrometry. Figures 5 and 6 illustrate the reconstructed ion chromatograms and mass fragmentograms of the F1 fraction from representative samples. Figure 7 illustrates the reconstructed ion chromatograms of the F3 fraction. The compounds identified in Core 167-1016C-1H are listed in Tables 1 and 2, and most of them were already reported by previous workers including Venkatesan et al. (1980), McEvoy et al. (1981), Simoneit and Manzurek (1981), Rullkötter et al. (1981), and Hinrichs et al. (1995). Concentrations of selected biomarkers and indices are shown in Appendixes A, and C through E.

Higher Plant-Derived Compounds

Long-chain *n*-alkanes (LNAs) occur as a major component of the F1 fraction in all investigated samples and maximize at C_{29} (Fig. 5). Their homologous distribution is typical of terrestrial higher plant waxes (Eglinton and Hamilton, 1967). The concentration of LNAs (*n*-C_{25}, *n*-C_{27}, *n*-C_{29}, and *n*-C_{31}) varies between 0.94 and 1.83 µg/g sediment, with an average of 1.43 µg/g sediment (Fig. 8). The variation with depth is small, but concentration minima occur at the warming intervals (0.6 and 8 mbsf). Their odd/even carbon number preference index (CPI) values (Bray and Evans, 1961) vary between 3.5 and 8.2, with an average of 5.4. The ratio of C_{31}/C_{27} of *n*-alkanes ranges between 1.3 and 2.7, with an average of 1.8. The small changes in CPI and C_{31}/C_{27} ratio suggest a homogenous source of *n*-alkanes.

According to the method of Prahl and Carpenter (1984), terrestrial organic carbon content (TROC) was calculated from LNA (*n*-C_{25}, *n*-C_{27}, *n*-C_{29}, and *n*-C_{31}) concentration (µg/g) using the following expression: TROC = LNA/(LNAr/TOCr), where LNAr and TOCr are the LNA and TOC of riverine sediments, respectively, that sourced terrigenous organic matter to the site. Because there are no available data for the LNAr/TOCr ratio of riverine sediments near Point Conception, we used the values from the Columbia River (Prahl and Carpenter, 1984). Based on this assumption, TROC (%) was expressed as LNA/2.77. Marine organic carbon content (MROC) was obtained by subtracting TROC from TOC. The estimated TROC is almost constant around 0.5%, whereas MROC varies between 0.4% and 2% (Fig. 8). The MROC decreases rapidly with depth in the top 9 cm, which reflects the degradation of metabolizable marine organic matter. MROC percentage of TOC ranges between 44.6% and 81.9%, with an average of 59.8%, which agrees with the low TOC/TN values of this core.

Diatom-Derived Compounds

$C_{25:4}$ and $C_{25:1}$ highly branched isoprenoid (HBI) alkenes were found in the F1 fraction. They were identified by comparison of their mass spectra and retention times (Requejo and Quinn, 1983). C_{25} HBI alkenes were identified in a marine diatom *Haslea ostrearia* (Volkman et al., 1994), and the compounds in sediments are thought to derive from diatoms.

$C_{25:4}$ HBI alkene decreases rapidly with increasing depth within top 60 cm of the core and is under the detection limit in the underlying horizons (Fig. 9). This implies that the $C_{25:4}$ HBI alkene is highly unstable during early diagenesis (Requejo and Quinn, 1983). In contrast, the $C_{25:1}$ HBI alkene seems more stable in the sediment column and has maximal concentrations in warming intervals (0.8 and 8 mbsf).

Haptophyte-Derived Compounds

C_{37}–C_{39} alkenones and C_{37}–C_{38} alkenoates (C_{36} fatty acid-methyl and ethyl esters) were found in the F3 fraction (Fig. 7), and C_{37}–C_{38} alkatrienes were found in the F1 fraction (Fig. 5). All of these in normal marine sediments are thought to derive from Genera *Gephyrocapsa* and *Emiliania,* Family Gephyrocasaceae, Class Haptophyceae (Marlowe et al., 1990).

Alkenones are most abundant in lipids extracted from Core 167-1016C-1H. Their concentrations vary between 2.0 and 16.5 µg/g sediment, with an average of 5.8 µg/g sediment, and have maximal values at 5.2, 6.2, and 7.4 mbsf (Fig. 10). Alkenoates have a similar variation with alkenones. Alkatrienes show a different variation with alkenones and alkenoates, and their concentrations are higher in a cooling interval (3.8–5.2 mbsf). Conte et al. (1994) compiled published and unpublished data for lipids in various strains of *Emiliania*

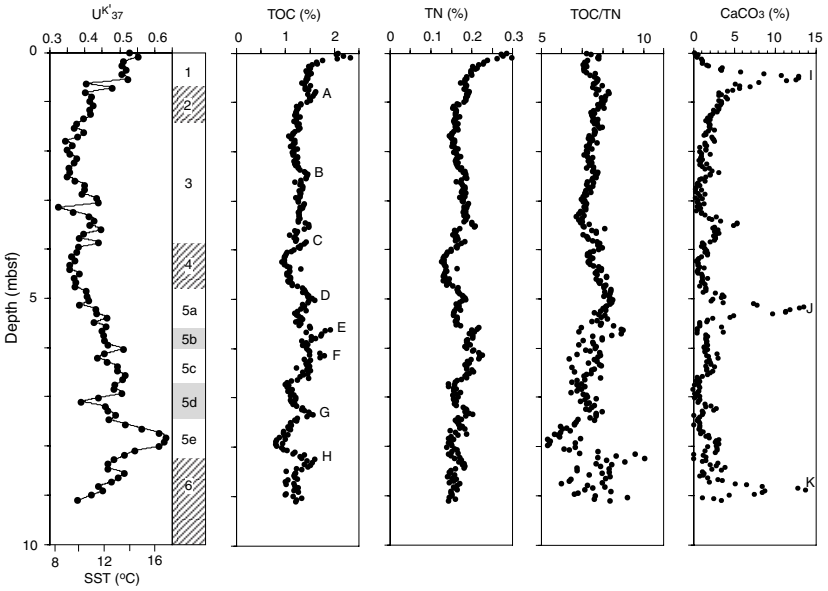

Figure 4. Total organic carbon (TOC), total nitrogen (TN), and calcium carbonate ($CaCO_3$) contents and TOC/TN ratio of Core 167-1016C-1H sediments. $U^{k'}_{37}$ profile is shown in comparison. Data are listed in Appendix B.

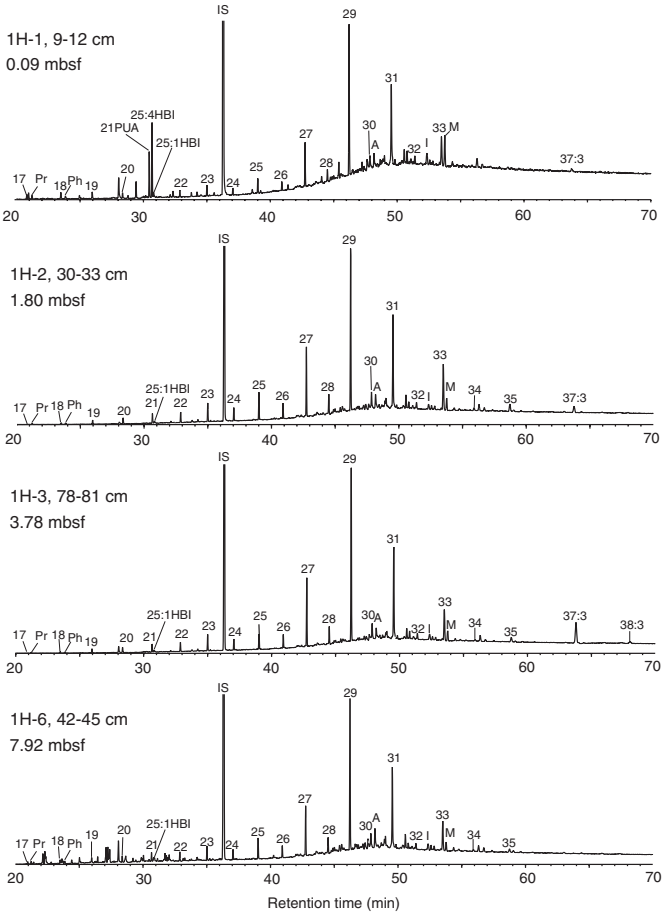

Figure 5. Reconstructed ion chromatograms of hydrocarbon (F1) fraction from Samples 167-1016C-1H-1, 9–12 cm, 167-1016C-1H-2, 30–33 cm, 167-1016C-1H-3, 78–81 cm, and 167-1016C-1H-6, 42–45 cm. The *n*-alkanes are marked with their carbon numbers. See Table 2 for a list of identified compounds. IS = internal standard (n-$C_{24}D_{50}$).

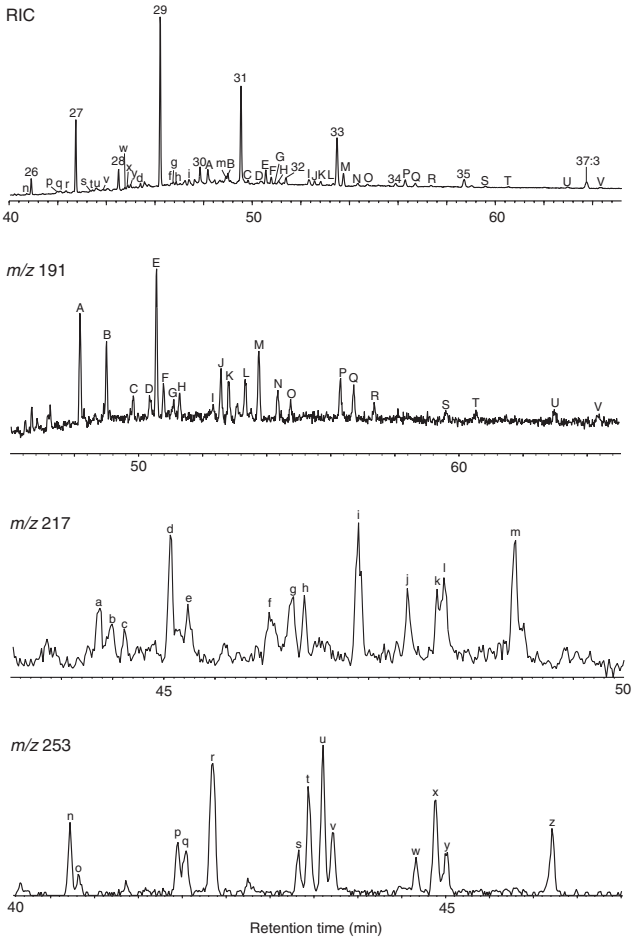

Figure 6. Partial reconstructed ion chromatogram and mass fragmentograms of *m/z* 191, 217, and 253 of hydrocarbon (F1) fraction from Sample 167-1016C-1H-2, 30–33 cm. See Table 1 for a list of identified compounds.

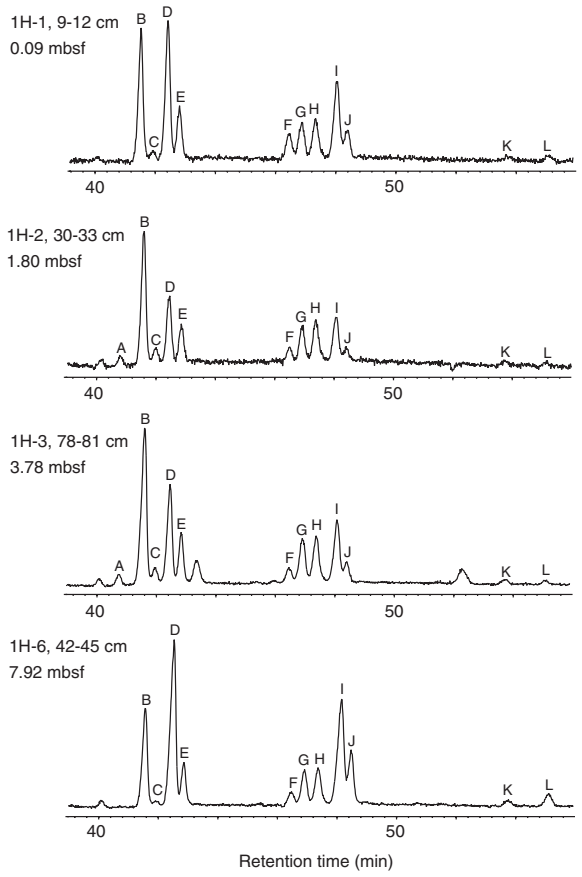

Figure 7. Partial reconstructed ion chromatograms of ketone (F3) fraction from Samples 167-1016C-1H-1, 9–12 cm, 167-1016C-1H-2, 30–33 cm, 167-1016C-1H-3, 78–81 cm, and 167-1016C-1H-6, 42–45 cm. See Table 2 for a list of identified compounds.

huxleyi and found that the occurrence of alkatrienes is restricted to several strains from northern subarctic Oceans such as the northeast Pacific Ocean and the English Channel. This suggests that the alkatrienes from Site 1016 reflect the contribution of *Emiliania* and/or *Gephyrocapsa* species of subarctic origin.

Prokaryote-Derived Compounds

In the F1 fraction, diploptene, neohop-13(18)-ene, and fern-7-ene were found, and hop-21(22)-ene and hop-17(21)-ene were detected in trace amounts (Fig. 6). All of these are thought to derive from eubacteria or cyanobacteria (Ourrison et al., 1979). Brassell et al. (1980) proposed a diagenetic isomerization of diploptene (hop-22(29)-ene) to neohop-13(18)-ene through hop-21(22)-ene and hop-17(21)-ene. There seems a trend that the relative abundance of neohop-13(18)-ene to diploptene increases with increasing depth (Fig. 9), which is consistent with the Brassell hypothesis. Both diploptene and neohop-13(18)-ene show similar variations with depth, but the amplitude is much higher in the variation of neohop-13(18)-ene concentration.

Petroleum-Type Compounds

Hopanes, steranes, and C-ring monoaromatic (MA) steroids were observed in the F1 fraction (Fig. 6). Their identification was achieved by comparison of their mass spectra and retention times (Philp, 1995; Moldowan and Fago, 1986; Schouten et al., 1994). Their isomeric pattern (e.g., the presence of thermally stable 22S- and 17α(H),

Table 1. Compounds identified in hydrocarbon (F1) fraction from Core 167-1016C-1H sediments.

Symbol	Compound
Pr	Pristane
Ph	Phytane
21PUA	C_{21} poly-unsaturated alkene
$C_{25:4}$HBI	$C_{25:4}$ highly branched isoprenoid alkene
$C_{25:1}$HBI	$C_{25:1}$ highly branched isoprenoid alkene
37:3	Heptatriacontatriene
38:3	Octatriacontatriene
A	17α(H),21β(H)-28,30-dinorhopane
B	17α(H),21β(H)-30-norhopane
C	17β(H),21α(H)-30-norhopane
D	Oleanane?
E	17α(H),21β(H)-hopane
F	Neohop-13(18)-ene
G	17β(H),21β(H)-30-norhopane
H	17β(H),21α(H)-hopane
I	Fern-7-ene
J	22S-17α(H),21β(H)-homohopane
K	22R-17α(H),21β(H)-homohopane
L	17β(H),21β(H)-hopane
M	Diploptene
N	22S-17α(H),21β(H)-bishomohopane
O	22R-17α(H),21β(H)-bishomohopane
P	17β(H),21β(H)-homohopane
Q	22S-17α(H),21β(H)-trishomohopane
R	22R-17α(H),21β(H)-trishomohopane
S	22S-17α(H),21β(H)-tetrakishomohopane
T	22R-17α(H),21β(H)-tetrakishomohopane
U	22S-17α(H),21β(H)-pentakishomohopane
V	22R-17α(H),21β(H)-pentakishomohopane
a	20S-5α(H),14α(H),17α(H)-cholestane
b	20R-5α(H),14β(H),17β(H)-cholestane
c	20S-5α(H),14β(H),17β(H)-cholestane
d	20R-5α(H),14α(H),17α(H)-cholestane
e	5α(H)-27-methyl-24-norcholestane
f	20S-5α(H),14α(H),17α(H)-24-methylcholestane
g	20R-5α(H),14β(H),17β(H)-24-methylcholestane
h	20S-5α(H),14β(H),17β(H)-24-methylcholestane
i	20R-5α(H),14α(H),17α(H)-24-methylcholestane
j	20S-5α(H),14α(H),17α(H)-24-ethylcholestane
k	20R-5α(H),14β(H),17β(H)-24-ethylcholestane
l	20S-5α(H),14β(H),17β(H)-24-ethylcholestane
m	20R-5α(H),14α(H),17α(H)-24-ethylcholestane
n	20S-5β(H),10β(CH_3)-C_{27} C-ring MA steroid
o	20S-5β(CH_3),10β(H)-C_{27} C-ring MA diasteroid
p	20R-5β(H),10β(CH_3)-C_{27} C-ring MA steroid
q	20S-5β(CH_3),10β(H)-C_{27} C-ring MA diasteroid
	20S-5α(H),10β(CH_3)-C_{27} C-ring MA steroid
r	20S-5β(H),10β(CH_3)-C_{28} C-ring MA steroid
	20S-5β(CH_3),10β(H)-C_{28} C-ring MA diasteroid
s	20R-5α(H),10β(CH_3)-C_{27} C-ring MA steroid
t	20S-5α(H),10β(CH_3)-C_{28} C-ring MA steroid
u	20R-5β(H),10β(CH_3)-C_{28} C-ring MA steroid
	20R-5β(CH_3),10β(H)-C_{28} C-ring MA diasteroid
v	20S-5β(H),10β(CH_3)-C_{29} C-ring MA steroid
	20S-5β(CH_3),10β(H)-C_{29} C-ring MA diasteroid
w	20S-5α(H),10β(CH_3)-C_{29} C-ring MA steroid
x	20R-5α(H),10β(CH_3)-C_{28} C-ring MA steroid
y	20R-5β(H),10β(CH_3)-C_{29} C-ring MA steroid
	20R-5β(CH_3),10β(H)-C_{29} C-ring MA diasteroid
z	20R-5α(H),10β(CH_3)-C_{29} C-ring MA steroid

Notes: MA = monoaromatic. The symbols refer to Figures 5 and 6.

Table 2. Compounds identified in ketone (F3) fraction from Core 167-1016C-1H sediments.

Symbol	Compound	Abbreviation
A	Heptatriaconta-8E,15E,22E,29E-tetraen-2-one	$C_{37:4}$MK
B	Heptatriaconta-8E,15E,22E-trien-2-one	$C_{37:3}$MK
C	Methylhexatriacontatrienoate	$C_{36:3}$ME
D	Heptatriaconta-15E,22E-dien-2-one	$C_{37:2}$MK
E	Methylhexatriacontadienoate	$C_{36:2}$ME
F	Ethylhexatriacontadienoate	$C_{36:2}$EE
G	Octatriaconta-9,16,23-trien-3-one	$C_{38:3}$EK
H	Octatriacontatrien-2-one	$C_{38:3}$MK
I	Octatriaconta-16,23-dien-3-one	$C_{38:2}$EK
J	Octatriacontadien-2-one	$C_{38:2}$MK
K	Nonatriacontatrien-3-one	$C_{39:3}$EK
L	Nonatriacontadien-3-one	$C_{39:2}$EK

Note: The symbols refer to Figure 7.

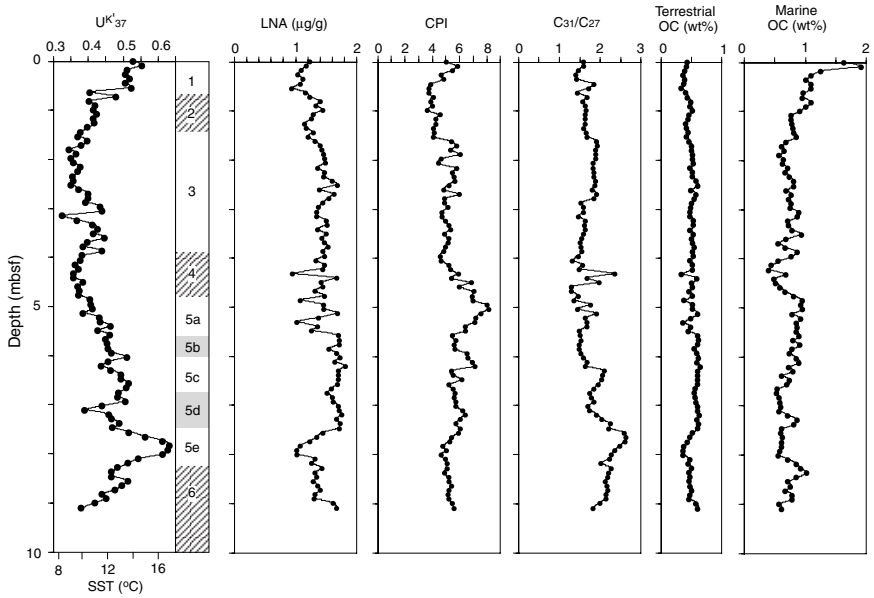

Figure 8. Concentration of long-chain *n*-alkanes (LNAs), C_{31}/C_{27} ratios of LNAs, odd/even carbon number preference index (CPI), and the terrestrial and marine organic carbon contents estimated from LNA concentrations in Core 167-1016C-1H sediments. $U^{k'}_{37}$ profile is shown in comparison. Data are listed in Appendix C.

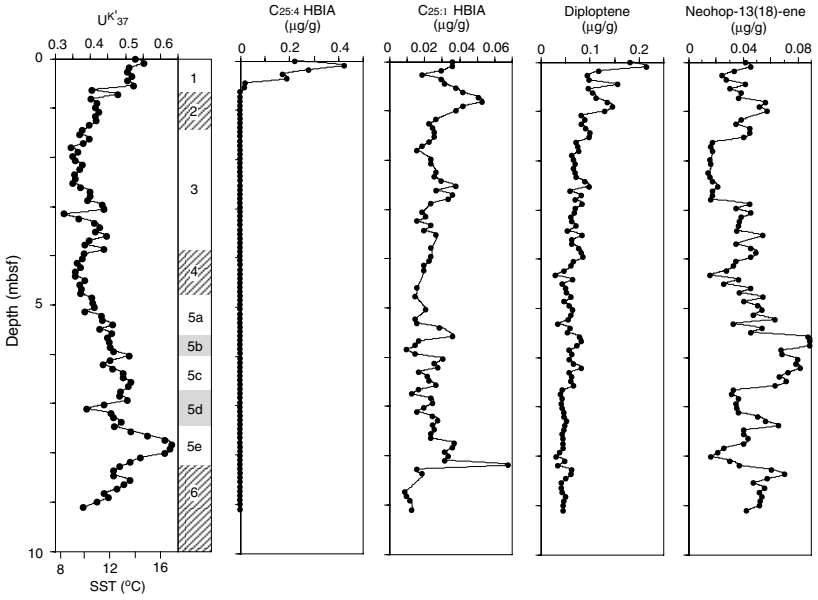

Figure 9. Concentrations of diatom-derived C_{25} highly branched isoprenoid alkenes (C_{25} HBIA) and prokaryote-derived diploptene and neohop-13(18)-ene in Core 167-1016C-1H sediments. $U^{k'}_{37}$ profile is shown in comparison. Data are listed in Appendix D.

21β(H)-hopanes and 20S- and 5α(H), 14β(H), 17β(H)-steranes) is typical of matured organic matter (Seifert and Moldowan, 1980), and the presence of 28, 30-dinorhopane (Seifert et al., 1978) implies that their source is a weathered Miocene Monterey Formation source rock and/or Monterey oil. Figure 11 demonstrates the variations in the concentrations of these petroleum-type compounds. All of these show parallel variations in concentration, and they are most abundant in warming intervals at 0.8 and 8.2 mbsf. The concentration of 28,30-dinorhopane ranges between 3 and 13 µg/g TOC, which is in the same order as that in Site 893 sediments in Santa Barbara Basin (10–42 µg/g TOC; Hinrichs et al., 1995).

DISCUSSION

Marine Ecological Responses to Climate Changes

The variations of TOC and $CaCO_3$ contents and biomarker concentrations appear to respond to glacial-interglacial changes. In this study, we used $C_{25:1}$ HBI alkene, alkenones, and neohop-13(18)-ene as the markers of diatoms, haptophytes, and prokaryotes, respectively, for assessing the marine ecological responses to climate changes.

The preservation degree of biomarkers in sediments depends both on the dissolved oxygen concentration near the water-sediment interface and sedimentation rate. A comparison of alkenone fluxes of sediment trap samples with those of sediments indicates that the preservation degree of alkenones is 0.25%–22% in oxic surface sediments off Oregon (Prahl et al., 1993). The biomarkers used in the present study are relatively stable, but even they could have suffered severe degradation in the water and sediment columns. Burrows were observed in whole range of Core 167-1016C-1H (Fig. 2), suggesting a constantly oxic environment during deposition. The sedimentation rates estimated from our preliminary $U^{k'}_{37}$ -based age-depth model are almost constant throughout the core. The little changes of bioturbation and constant sedimentation rate suggest that only small variations occurred in the degree of preservation of biomarkers during the deposition of the core. It is, therefore, possible to use the relative abundance of the biomarkers for paleoenvironmental assessment.

A comparison of TOC and $CaCO_3$ contents with selected biomarker concentrations is shown in Figure 12. $C_{25:1}$ HBI alkene of diatom origin has the highest concentrations in warming intervals (Peaks A and H in Fig. 12). Pike et al. (unpubl. data) point out the increase of diatom productivity at deglaciation (Termination I) at Site 1019 off Oregon, based on the diatom assemblages and the mode of lamination. This is concordant with the high $C_{25:1}$ HBI alkene concentrations during warming intervals at Site 1016, implying the regional increase of diatom productivity at deglaciation along the California and Oregon margins. The high diatom productivity (high concentration of $C_{25:1}$ HBI alkene) was presumably related to intensified coastal upwelling and accounts for major peaks of TOC contents (Peaks A and H).

Alkenones of haptophyte origin, in contrast, have maximal concentrations in the cooling intervals of the warm period (Peaks D, F, and G in Fig. 12). The alkenone maxima correspond to the maximal peaks of TOC contents. This implies that alkenone-producing haptophyte algae, in addition to diatoms, are major sources of marine organic carbon. It is interesting to note that the concentrations of alkenones and $C_{25:1}$ HBI alkene vary out of phase in a warm interval (5–8 mbsf). Because diatoms tend to dominate in a highly nutrient-fluctuating environment (Turpin and Harrison, 1979), the out-of-phase variations presumably resulted from the changes in the mode of nutrient supply to surface mixed layer, such as the changes of the intensity, seasonality, frequency, or duration of upwelling.

Neohop-13(18)-ene of prokaryote origin has maximal concentrations mostly at the maximal intervals of diatom-derived $C_{25:1}$ HBI alkene and haptophyte-derived alkenone concentrations (Fig. 12). Because neohop-13(18)-ene derives from bacteria or cyanobacteria, its concentration reflects either heterotrophic eubacterial activity or productivity of cyanobacteria and/or autotrophic eubacteria. The synchronous variation of neohop-13(18)-ene with $C_{25:1}$ HBI alkene and alkenones, therefore, suggests that this compound reflects heterotrophic eubacterial activity associated with the primary production by diatoms and haptophytes. The possibility of autotrophic origin, however, cannot be neglected at present, and therefore a future investigation on its carbon isotopic composition is desirable to identify its source.

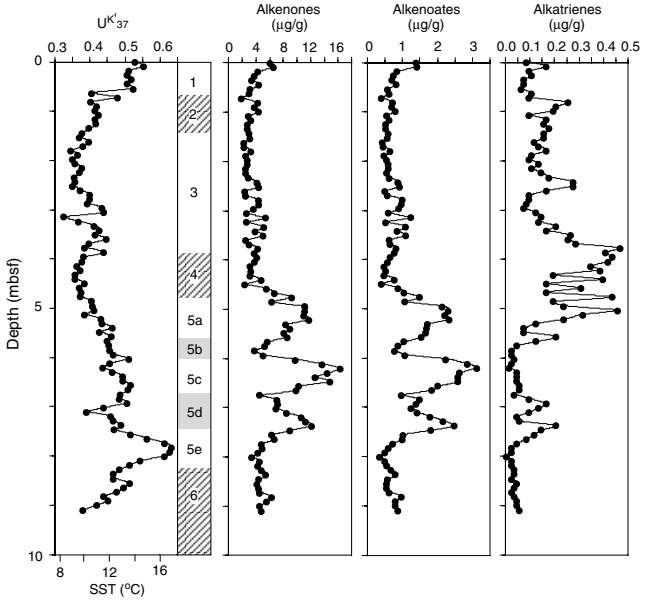

Figure 10. Concentrations of haptophyte-derived alkenones, alkenoates, and alkatrienes in Core 167-1016C-1H sediments. $U^{k'}_{37}$ profile is shown in comparison. Data are listed in Appendix A.

Carbonate Dissolution Changes

Maximal $CaCO_3$ contents (>10%) were observed in warming intervals (Peaks I and K in Fig. 12) and a cooling interval (Peak J). There is no biomarker that varies in phase with carbonate Peaks I and K in the warming intervals. On the other hand, Peak J of the cooling interval corresponds to an alkenone maximum, implying that high haptophyte productivity is related to carbonate maxima. These suggest that the processes that regulate the formation of carbonate peaks are different between warming and cooling intervals.

The background value of $CaCO_3$ contents is nearly 0%, which suggests routine dissolution of calcium carbonate below the CCD. The changes of CCD are controlled mainly both by the changes of North Pacific deep-water chemistry and local flux of calcium carbonate. The out-of-phase responses of the Atlantic and Pacific carbonate records to climate change were attributed to a global mechanism (i.e., an increased contribution of less corrosive southern source water and decreased input of corrosive North Atlantic Deep Water during glacial periods [Berger, 1970]). Karlin et al. (1992), however, suggested that the CCD has migrated more than 1800 m between glacial and interglacial times, and they attributed this large carbonate fluctuation to

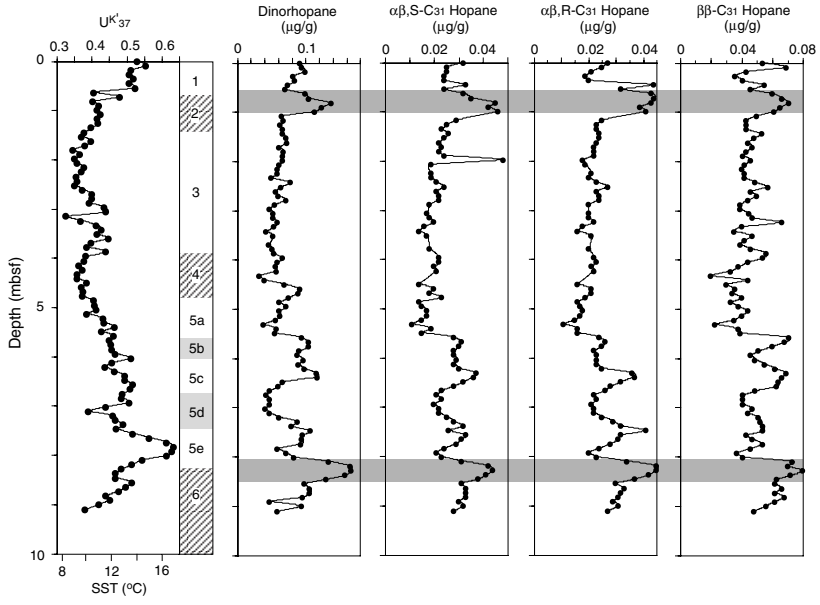

Figure 11. Concentrations of petroleum-type compounds in Core 167-1016C-1H sediments. $U^{k'}_{37}$ profile is shown in comparison. Data are listed in Appendix E.

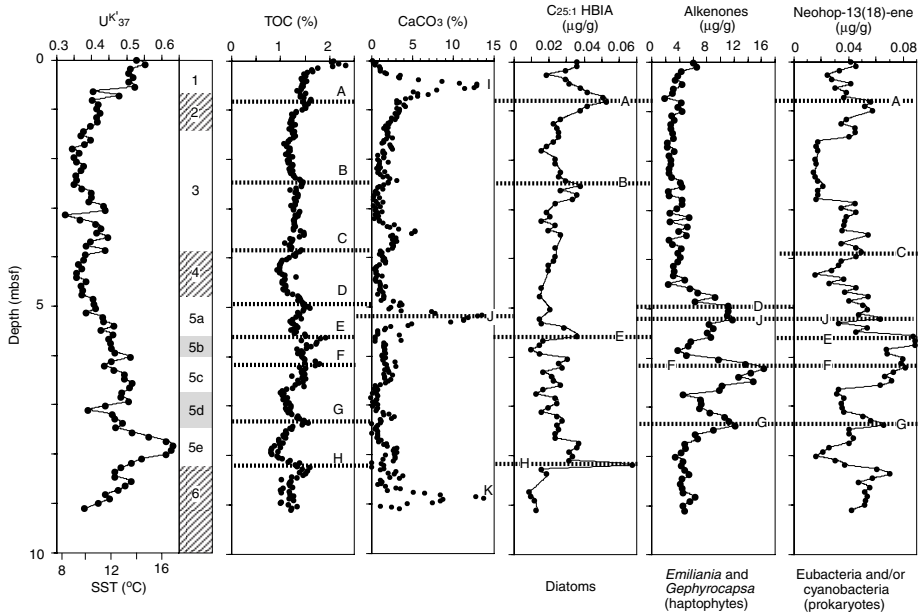

Figure 12. Correlations of TOC and $CaCO_3$ contents with biomarker concentrations in Core 167-1016C-1H. $U^{k'}_{37}$ profile is shown in comparison.

some regional mechanisms, such as the glacial deep-water formation in the northern Pacific Ocean or the enhanced dissolution caused by interglacial noncarbonate productivity related to coastal upwelling. Gardner et al. (1997) found a carbonate preservation event at 10 ka in cores from the northern California margin, and they attributed it to the global mechanism, which was hypothesized by Broecker et al. (1993), that the expansion of boreal forests in northern hemisphere removed CO_2 from the atmosphere and the surface water of the ocean, and in turn increased alkalinity of ocean water, which should have resulted in greater preservation of calcium carbonate.

On the other hand, the local flux of calcium carbonate can be examined based on the alkenone profile. Because alkenone-producing species compose more than 70% of total coccoliths at the adjacent Site 1017 (Tanaka and Tada, Chap. 27, this volume), it is reasonable to use alkenone concentrations to estimate the flux of calcium carbonate. Carbonate Peak J corresponds to an alkenone maximum (Fig. 12), which is concordant with the hypothesis that increased calcium carbonate production enhances its preservation. However, during the older cooling intervals (6–8 mbsf), there is no carbonate maximum that corresponds to alkenone maxima, implying that the production is not the only factor controlling CCD at this site.

According to the model of Archer (1991), the dissolution of calcium carbonate is controlled by organic carbon/carbonate carbon ratio of sinking particles, and this implies that the production of noncarbonate organisms such as diatoms tends to decrease the preservation of calcium carbonate. At Site 1016, both TOC content and $C_{25:1}$ HBI alkene concentration are low at carbonate maxima (>10%), and this does not disagree with the Archer hypothesis.

Lyle et al. (Chap. 11, this volume) report the synchronous changes in calcium carbonate contents and accumulation rates in various water depths at northern sites of Leg 167 and suggest that the carbonate profiles are affected by carbonate production rather than dissolution. Site 1017, adjacent to Site 1016, shows a maximum of total coccolith abundance during early Holocene (Tanaka and Tada, Chap. 27, this volume). This might suggest that calcium carbonate production controls its preservation in the Sites 1016–1017 transect too. However, alkenones have no maximal concentration at carbonate maxima (Peaks I and K) of Site 1016 (Fig. 12): the alkenone profile of Site 1016 provides no concrete evidence that carbonate production mainly affects carbonate profile. To answer this question, a future investigation is needed about the alkenone profile at Site 1017.

We therefore still need to consider the regional factors at a northern Pacific scale (Karlin et al., 1992) or the global factors (Broecker et al., 1993). It is interesting to note that the calcium carbonate profile of a deep-sea core (4402 m deep) from the Caroline Basin, the western equatorial Pacific Ocean (Kawahata et al., 1998), somewhat resembles that of Site 1016. This suggests the importance of understanding the changes of deep-water chemistry of the northern Pacific Ocean to account for CCD changes in the California margin.

Sources and Transportation of Petroleum-Type Compounds

Petroleum-type compounds have been widely observed in recent sediments of the California Borderland, and they have been attributed to anthropogenic petroleum pollution as well as to input from natural sources such as submarine seep oil and weathered Monterey shales (Simoneit and Kaplan, 1980; Venkatesan et al., 1980). They were also detected in sinking particles taken by sediment traps settled in the California Borderland (Crisp et al., 1979; Venkatesan and Kaplan, 1992). A 3-cm-thick tar layer and small tar fragments were observed in Site 893 cores from the Santa Barbara Basin (Shore-based Scientific Party, 1994). Hinrichs et al. (1995) found petroleum-type compounds in late Pleistocene sediments (since 160 ka) from Site 893, and it indicated that they are solely of natural origin in older sediments.

Petroleum-type compounds were observed in Site 1016 sediments in this study, indicating that the occurrence of petroleum-type compounds of natural origin is not restricted to coastal sediments but extends to hemipelagic deep-sea sediments. The generation of petroleum in deeper parts of Site 1016 is very unlikely because of the low TOC contents (0.5%–1%) in the underlying sediments (Shipboard Scientific Party, 1997a). The presence of compounds characteristic of Monterey shales and Monterey oils indicates that their potential sources are Miocene Monterey shales exposed along the California coastal area (Pisciotto and Garrison, 1981) and/or natural seep oil in the California Borderland (Vernon and Slater, 1963).

The variation of long-chain *n*-alkane concentrations at Site 1016 indicates relatively low contribution of terrigenous organic matter in warming intervals (Fig. 8). On the other hand, the concentrations of petroleum-type compounds are higher in warming intervals (Fig. 11). This observation disagrees with the idea of terrestrial origin of petro-

leum-type compounds such as weathered Monterey shales on land. Therefore, a submarine origin is more likely.

Submarine petroleum seepages were recognized on the continental shelves of the California Borderland (e.g., Wilson et al., 1974). Natural seeps off Coal Oil Point introduce about 50 to 70 barrels of oil per day into the Santa Barbara Basin (Allen et al., 1970). There are three huge tar mounds that resulted from the accumulation of altered seep oil in the Santa Barbara Basin (Vernon and Slater, 1963). The tar mounds, built on land during the last glacial period, were washed away once by wave activities during transgression and then rebuilt in water during the Holocene (Vernon and Slater, 1963). Therefore, it is proposed that a huge amount of tar was scattered to the surrounding areas by the destruction of tar mounds during transgression. The timing of destruction of tar mounds corresponds to the periods of maximum input of petroleum-type compounds into Site 1016. The biggest tar mound is located off Point Conception (Vernon and Slater, 1963), and this area is very close to the Arguello Canyon, which sources sediments to the Arguello Fan (Chase et al., 1981). Because the lobe of the Arguello Fan extends to the south of Site 1016, a turbidity current is a possible candidate for transporting tarry materials to deep seafloor, and the deposition of the tarry turbidite sediments presumably contributed to the accumulation of petroleum-type compounds at Site 1016. Although the other transportation mechanisms such as diffusion and floating cannot be neglected, the same level of their concentrations in Site 1016 as in the Santa Barbara Basin suggests that the transportation by turbidity currents is more likely.

CONCLUSIONS

TOC and $CaCO_3$ contents were determined for 304 samples, and biomarkers were analyzed for 101 samples from Core 167-1016C-1H.

Paleotemperature estimated from $U^{k'}_{37}$ varies from 8.5° to 17.5°C. The $U^{k'}_{37}$ variation implies that Core 167-1016C-1H covers oxygen isotope Stages 1–6, with an average linear sedimentation rate of 6.4 cm/k.y.

The responses of marine ecosystem to glacial-interglacial climate changes are evident in the variations of TOC, $CaCO_3$, and biomarker concentrations. Peaks of diatom-derived $C_{25:1}$ HBI alkene concentrations occur during warming intervals, suggesting intensified upwelling during deglaciation. The concentrations of haptophyte-derived alkenones and diatom-derived $C_{25:1}$ HBI alkene vary out of phase, which presumably resulted from the changes in the mode of nutrient supply to surface mixed layer, such as the changes of the intensity, seasonality, frequency, or duration of upwelling.

Maximal $CaCO_3$ contents (>10%) were observed in both warming and cooling intervals. The peak in cooling interval relates to an alkenone maximum, whereas the peaks in warming intervals do not. This implies that carbonate production is not the only factor controlling CCD at this site and suggests considering the importance of changes of North Pacific deep-water chemistry.

Petroleum-type compounds are present in Site 1016 sediments, indicating that their occurrence is not restricted to coastal sediments, but extends to hemipelagic deep-sea sediments. The concentrations of petroleum-type compounds maximize in the warming intervals that correspond to the timing of destruction of a huge tar mound off Point Conception. They were presumably transported by the Arguello Fan system to Site 1016.

ACKNOWLEDGMENTS

We thank Ms. Kazuko Hino for analytical assistance in the laboratory. Special thanks are due to Drs. Yuichiro Tanaka and Masatoshi Komiya, for valuable discussion. Also, thanks are extended to shore-based sampling participants for help in our sampling. The helpful reviews by P.A. Meyers and A. Miller improved the quality of this manuscript. This study was financially supported by the Science and Technology Agency of Japan.

REFERENCES

Allen, A.A., Schlueter, R.S., and Mikolaj, P.G., 1970. Natural oil seepage at Coal Oil Point, Santa Barbara, California. *Science,* 170:974–977.

Archer, D., 1991. Modeling the calcite lysocline. *J. Geophys. Res.,* 96:17037–17050.

Berger, W.H., 1970. Planktonic foraminifera: selective solution and the lysocline. *Mar. Geol.,* 8:111–138.

Berger, W.H., Lange, C.B., and Weinheimer, A., 1997. Silica depletion of the thermocline in the eastern North Pacific during glacial conditions: clues from Ocean Drilling Program Site 893, Santa Barbara Basin, California. *Geology,* 25:619–622.

Brassell, S.C., Brereton, R.G., Eglinton, G., Grimalt, J., Liebezeit, G., Marlower, I.T., Pfaumann, U., and Sarntheim, M., 1986. Palaeoclimatic signals recognised by chemometric treatment of molecular stratigraphic data. *In* Leythaeuser, D., and Rullkötter, J. (Eds.), *Advances in Organic Geochemistry 1985.* Org. Geochem., 10:649–660.

Brassell, S.C., Comet, P.A., Eglinton, G., Isaacson, P.J., McEvoy, J., Maxwell, J.R., Thomson, I.D., Tibbetts, P.J., and Volkman, J.K., 1980. The origin and fate of lipids in the Japan Trench. *In* Douglas, A.G., and Maxwell, J.R. (Eds.), *Advances in Organic Geochemistry 1979:* Oxford (Pergamon Press), 375–392.

Bray, E.E., and Evans, E.D., 1961. Distribution of *n*-paraffins as a clue to recognition of source beds. *Geochim. Cosmochim. Acta,* 22:2–15.

Broecker, W.S., Lao, Y., Klas, M., and Clark, E., 1993. A search for early Holocene $CaCO_3$ preservation event. *Paleoceanography,* 8:333–339.

Chase, T.E., Wilde, P., Normark, W.R., Miller, C.P., Seekins, B.A., and Young, J.D., 1981. Offshore topography of the western United States between 32° and 42° north latitudes. *U.S. Geol. Surv. Open-File Map,* 81-443.

Conte, M.H., Volkman, J.K., and Eglinton, G., 1994. Lipid biomarkers of Haptophyta. *In* Green, J.C., and Leadbeater, B.S.C. (Eds.), *The Haptophyte Algae:* Oxford (Clarendon Press), 351–377.

Crisp, P.T., Brenner, S., Venkatesan, M.I., Ruth, E., and Kaplan, I.R., 1979. Organic chemical characterization of sediment-trap particulates from San Nicolas, Santa Barbara, Santa Monica, and San Pedro Basins, California. *Geochim. Cosmochim. Acta,* 43:1791–1801.

Dean, W.E., Gardner, J.V., and Piper, D.Z, 1997. Inorganic geochemical indicators of glacial-interglacial changes in productivity and anoxia on the California continental margin. *Geochim. Cosmochim. Acta,* 61:4507–4518.

Doose, H., Prahl, F.G., and Lyle, M.W., 1997. Biomarker temperature estimates for modern and last glacial surface waters of the California Current system between 33° and 42°N. *Paleoceanography,* 12:615–622.

Eglinton, G., and Hamilton, R.J., 1967. Leaf epicuticular waxes. *Science,* 156:1322–1335.

Gardner, J.V., and Dartnell, P., 1995. Centennial-scale late Quaternary stratigraphies of carbonate and organic carbon from Santa Barbara Basin, Hole 893A, and their paleoceanographic significance. *In* Kennett, J.P., Baldauf, J.G., and Lyle, M. (Eds.), *Proc. ODP, Sci. Results,* 146 (Pt. 2): College Station, TX (Ocean Drilling Program), 103–124.

Gardner, J.V., Dean, W.E., and Dartnell, P., 1997. Biogenic sedimentation beneath the California Current system for the past 30 kyr and its paleoceanographic significance. *Paleoceanography,* 12:207–225.

Hedges, J.I., and Mann, D.C., 1979. The lignin geochemistry of marine sediments from the southern Washington coast. *Geochim. Cosmochim. Acta,* 43:1809–1818.

Herbert, T.D., Schuffert, J.D., Thomas, D., Lange, K., Weinheimer, A., Peleo-Alampay, A., and Herguera, J.-C., 1998. Depth and seasonality of alkenone production along the California margin inferred from a core-top transect. *Paleoceanography,* 13:263–271.

Herbert, T.D., Yasuda, M., and Burnett, C., 1995. Glacial-interglacial sea-surface temperature record inferred from alkenone unsaturation indices, Site 893, Santa Barbara Basin. *In* Kennett, J.P., Baldauf, J.G., and Lyle, M. (Eds.), *Proc. ODP, Sci. Results,* 146 (Pt. 2): College Station, TX (Ocean Drilling Program), 257–264.

Heusser, L.E., 1995. Pollen stratigraphy and paleoecologic interpretation of the 160-k.y. record from Santa Barbara Basin, Hole 893A. *In* Kennett, J.P., Baldauf, J.G., and Lyle, M. (Eds.), *Proc. ODP, Sci. Results,* 146 (Pt. 2): College Station, TX (Ocean Drilling Program), 265–279.

Hickey, B.M., 1979. The California Current System: hypotheses and facts. *Prog. Oceanogr.,* 8:191–279.

Hinrichs, K.-U., Rinna, J., Rullkötter, J., and Stein, R., 1997. A 160 kyr record of alkenone-derived sea-surface temperatures from Santa Barbara basin sediments. *Naturwissenschaften,* 84:126–128.

Hinrichs, K.-U., Rullkötter, J., and Stein, R., 1995. Preliminary assessment of organic geochemical signals in sediments from Hole 893A, Santa Barbara Basin, offshore California. *In* Kennett, J.P., Baldauf, J.G., and Lyle, M. (Eds.), *Proc. ODP, Sci. Results,* 146 (Pt. 2): College Station, TX (Ocean Drilling Program), 201–211.

Huyer, A., 1983. Coastal upwelling in the California Current system. *Prog. Oceanogr.,* 12:259–284.

Kahn, M.I., Oba, T., and Ku, T.-L., 1981. Paleotemperatures and glacially induced changes in the oxygen-isotope composition of seawater during the late Pleistocene and Holocene time in Tanner Basin, California. *Geology,* 9:485–490.

Karlin, R., Lyle, M., and Zahn, R., 1992. Carbonate variations in the Northeast Pacific during the late Quaternary. *Paleoceanography,* 7:43–61.

Kawahata, H., Suzuki, A., and Ahagon, N., 1998. Biogenic sediments in the West Caroline Basin, the western equatorial Pacific during the last 330,000 years. *Mar. Geol.,* 149:155–176.

Kennedy, J.A., and Brassell, S.C., 1992. Molecular stratigraphy of the Santa Barbara basin: comparison with historical records of annual climate change. *Org. Geochem.,* 19:235–244.

Kennett, J.P., and Ingram, B.L., 1995. A 20,000-year record of ocean circulation and climate change from the Santa Barbara Basin. *Nature,* 377:510–512.

Kennett, J.P., and Venz, K., 1995. Late Quaternary climatically related planktonic foraminiferal assemblage changes: Hole 893A, Santa Barbara Basin, California. *In* Kennett, J.P., Baldauf, J.G., and Lyle, M. (Eds.), *Proc. ODP, Sci. Results,* 146 (Pt. 2): College Station, TX (Ocean Drilling Program), 281–293.

Louda, J.W., and Baker, E.W., 1981. Geochemistry of tetrapyrrole, carotenoid, and perylene pigments in sediments from the San Miguel Gap (Site 467) and Baja California borderland (Site 471), Deep Sea Drilling Project Leg 63. *In* Yeats, R.S., Haq, B.U., et al., *Init. Repts. DSDP,* 63: Washington (U. S. Govt. Printing Office), 785–818.

Lyle, M., Zahn, R., Prahl, F., Dymond, J., Collier, R., Pisias, N., and Suess, E., 1992. Paleoproductivity and carbon burial across the California Current: the Multitracers Transect, 42°N. *Paleoceanography,* 7:251–272.

Lynn, R.J., and Simpson, J.J., 1987. The California Current system: the seasonal variability of its physical characteristics. *J. Geophys. Res.,* 92:12947–12966.

Marlowe, I.T., Brassell, S.C., Eglinton, G., and Green, J.C., 1990. Long-chain alkenones and alkyl alkenoates and the fossil coccolith record of marine sediments. *Chem. Geol.,* 88:349–375.

McEvoy, J., Eglinton, G., and Maxwell, J.R., 1981. Preliminary lipid analyses of sediments from Sections 467-3-3 and 467-97-2. *In* Yeats, R.S., Haq, B.U., et al., *Init. Repts. DSDP,* 63: Washington (U.S. Govt. Printing Office), 763–774.

Moldowan, J.M., and Fago, F., 1986. Structure and significance of a novel rearranged monoaromatic steroid hydrocarbon in petroleum. *Geochim. Cosmochim. Acta,* 50:343–351.

Mortyn, P.G., and Thunell, R.C., 1997. Biogenic sedimentation and surface productivity changes in the Southern California Borderlands during the last glacial-interglacial cycle. *Mar. Geol.,* 138:171–192.

Mortyn, P.G., Thunell, R., Anderson, D., Stott, L., and Le, J., 1996. Sea surface temperature changes in the Southern California Borderlands during the last glacial-interglacial cycle. *Paleoceanography,* 11:415–430.

Ortiz, J., Mix, A., Hostetler, S., and Kashgarian, M., 1997. The California Current of the last glacial maximum: reconstruction at 42 degrees N based on planktonic foraminifera. *Paleoceanography,* 12:191–205.

Ourisson, G., Albrecht, P., and Rohmer, M., 1979. The hopanoids: paleochemistry and biochemistry of a group of natural products. *Pure Appl. Chem.,* 51:709–729.

Parsons, T.R., Takahashi, M., and Hargrove, B., 1984. *Biological Oceanographic Processes* (3rd ed.): New York (Pergamon Press).

Philp, R.P., 1985. Fossil fuel biomarkers: applications and spectra. *Meth. Geochem. Geophys.,* 23.

Pisciotto, K.A., and Garrison, R.E., 1981. Lithofacies and depositional environments of the Monterey Formation, California. *In* Garrison, R.E., and Douglas, R.G. (Eds.), *The Monterey Formation and Related Siliceous Rocks of California.* Spec. Publ.—Pacific Sec. Soc. Econ. Paleontol. Mineral., 97–122.

Prahl, F.G., and Carpenter, R., 1984. Hydrocarbons in Washington coastal sediments. *Estuarine Coastal Shelf Sci.,* 18:703–720.

Prahl, F.G., Collier, R.B., Dymond, J., Lyle, M., and Sparrow, M.A., 1993. A biomarker perspective on prymnesiophyte productivity in the northeast Pacific Ocean. *Deep-Sea Res. Part A,* 40:2061–2076.

Prahl, F.G., Muehlhausen, L.A., and Zahnle, D.L., 1988. Further evaluation of long-chain alkenones as indicators of paleoceanographic conditions. *Geochim. Cosmochim. Acta,* 52:2303–2310.

Prahl, F.G., Pisias, N., Sparrow, M.A., and Sabin, A., 1995. Assessment of sea-surface temperature at 42° N in the California Current over the last 30,000 years. *Paleoceanography,* 10:763–773.

Prahl, F.G., and Wakeham, S.G., 1987. Calibration of unsaturation patterns in long-chain ketone compositions for paleotemperature assessment. *Nature,* 330:367–369.

Requejo, A.G., and Quinn, J.G., 1983. Geochemistry of C_{25} and C_{30} biogenic alkenes in sediments of the Narragansett Bay estuary. *Geochim. Cosmochim. Acta,* 47:1075–1090.

Robinson, M.M., 1976. *Atlas of the North Pacific Ocean: Monthly Mean Temperature and Mean Salinities of the Surface Layer:* Washington, D.C. (Naval Oceanographic Office).

Roemmich, D., and McGown, J., 1995. Climatic warming and the decline of zooplankton in the California Current. *Science,* 267:1324–1326.

Rullkötter, J., von der Dick, H., and Welte, D.H., 1981. Organic petrography and extractable hydrocarbons of sediments from the eastern North Pacific Ocean, Deep Sea Drilling Project Leg 63. *In* Yeats, R.S., Haq, B.U., et al., *Init. Repts. DSDP,* 63: Washington (U.S. Govt. Printing Office), 819–836.

Sancetta, C., Lyle, M., Heusser, L., Zahn, R., and Bradbury, J.P., 1992. Late-glacial to Holocene changes in winds, upwelling, and seasonal production of the Northern California current system. *Quat. Res.,* 38:359–370.

Schouten, S., Sinninghe Damsté, J.S., Schoell, M., and de Leeuw, J.W., 1994. A novel sterane, 27-nor-24-methyl-5 ±-cholestane, in sediments. *Geochim. Cosmochim. Acta,* 58:3741–3745.

Seifert, W.K., and Moldowan, J.M., 1980. The effect of thermal stress on source-rock quality as measured by hopane stereochemistry. *Phys. Chem. Earth,* 12:229–237.

Seifert, W.K., Moldowan, J.M., Smith, G.W., and Whitehead, E.V., 1978. First proof of structure of a C_{28}-pentacyclic triterpane in petroleum. *Nature,* 271:436–437.

Shipboard Scientific Party, 1997a. Site 1016. *In* Lyle, M., Koizumi, I., Richter, C., et al., *Proc. ODP, Init. Repts.,*167: College Station, TX (Ocean Drilling Program), 239–283.

————, 1997b. Site 1017. *In* Lyle, M., Koizumi, I., Richter, C., et al., *Proc. ODP, Init. Repts.,*167: College Station, TX (Ocean Drilling Program), 285–309.

Shore-based Scientific Party, 1994. Site 893. *In* Kennett, J.P., Baldauf, J.G., et al., *Proc. ODP, Init. Repts.,* 146 (Pt. 2): College Station, TX (Ocean Drilling Program), 15–50.

Simoneit, B.R.T., 1977. Diterpenoid compounds and other lipids in deep-sea sediments and their geochemical significance. *Geochim. Cosmochim. Acta,* 41:463–476.

Simoneit, B.R.T., and Kaplan, I.R., 1980. Triterpenoids as molecular indicators of paleoseepage in Recent sediments of the Southern California Bight. *Mar. Environ. Res.,* 3:113–128.

Simoneit, B.R.T., and Mazurek, M.A., 1981. Organic geochemistry of sediments from the southern California Borderland, Deep Sea Drilling Project Leg 63. *In* Yeats, R.S., Haq, B.U., et al., *Init. Repts. DSDP,* 63: Washington (U.S. Govt. Printing Office), 837–853.

Stein, R., and Rack, F.R., 1995. A 160,000-year high-resolution record of quantity and composition of organic carbon in the Santa Barbara Basin (Site 893). *In* Kennett, J.P., Baldauf, J.G., and Lyle, M. (Eds.), *Proc. ODP, Sci. Results,* 146 (Pt. 2): College Station, TX (Ocean Drilling Program), 125–138.

Thunell, R.C., and Mortyn, P.G., 1995. Glacial climate instability in the Northeast Pacific Ocean. *Nature,* 376:504–506.

Turpin, D.H., and Harrison, P.J., 1979. Limiting nutrient patchiness and its role in phytoplankton ecology. *J. Exp. Mar. Biol. Ecol.,* 39:151–166.

Venkatesan, M.I., Brenner, S., Ruth, E., Bonilla, J., and Kaplan, I.R., 1980. Hydrocarbons in age-dated sediment cores from two basins in the Southern California Bight. *Geochim. Cosmochim. Acta,* 44:789–802.

Venkatesan, M.I., and Kaplan, I.R., 1992. Vertical and lateral transport of organic carbon and the carbon budget in Santa Monica Basin, California. *Prog. Oceanogr.,* 30:291–312.

Venkatesan, M.I., Ruth, E., and Kaplan, I.R., 1990. Triterpenols from sediments of Santa Monica Basin, Southern California Bight, U.S.A. *Org. Geochem.,* 16:1015–1024.

Vernon, J.W., and Slater, R.A., 1963. Submarine tar mound, Santa Barbara County, California. *AAPG Bull.,* 47:1624–1627.

Volkman, J.K., Barrett, S.M., and Dunstan, G.A., 1994. C_{25} and C_{30} highly branched isoprenoids in laboratory cultures of two marine diatoms. *Org. Geochem.,* 21:407–414.

Wilson, R.D., Monaghan, P.H., Osanik, A., Price, L.C., and Rogers, M.A., 1974. Natural marine oil seepage. *Science,* 184:857–865.

Yamamuro, M., and Kayanne, H., 1995. Rapid direct determination of organic carbon and nitrogen in carbonate bearing sediments using Yanaco MT-5 CHN analyzer. *Limnol. Oceanogr.,* 39:1726–1733.

Date of initial receipt: 14 October 1998
Date of acceptance: 15 June 1999
Ms 167SR-224

Appendix A. Concentrations and unsaturation indices of alkenones and alkenoates in Core 167-1016C-1H sediments.

Core, section, interval (cm)	Depth (mbsf)	$U^{K'}_{37}$	SST (°C)	U^{me}_{36}	$K_{37:4}/K_{37}$	Alkenones (µg/g)	Alkenoates (µg/g)	Alkatrienes (µg/g)
167-1016C-								
1H-1, 0-3	0.00	0.53	14.5	0.85	0.000	6.19	1.41	0.094
1H-1, 9-12	0.09	0.55	15.2	0.85	0.000	6.70	1.45	0.168
1H-1, 18-21	0.18	0.51	13.9	0.83	0.000	4.40	0.89	0.102
1H-1, 27-30	0.27	0.51	13.8	0.84	0.000	3.92	0.78	0.106
1H-1, 36-39	0.36	0.52	14.2	0.85	0.000	3.58	0.72	0.081
1H-1, 45-48	0.45	0.51	13.8	0.85	0.010	4.57	0.84	0.082
1H-1, 54-57	0.54	0.53	14.3	0.85	0.011	3.33	0.59	0.065
1H-1, 63-66	0.63	0.41	10.8	0.78	0.036	3.19	0.65	0.106
1H-1, 72-75	0.72	0.48	13.0	0.81	0.026	2.01	0.42	0.095
1H-1, 81-84	0.81	0.40	10.8	0.76	0.049	4.36	0.76	0.262

This is a sample of the table that appears on the volume CD-ROM.

Appendix B. Total carbon, total organic carbon, inorganic carbon, total nitrogen, and calcium carbonate contents and TOC/TN ratio of Core 167-1016C-1H sediments.

Core, section, interval (cm)	Depth (mbsf)	TC (%)	TOC (%)	IC (%)	$CaCO_3$ (%)	TN (%)	TOC/TN
167-1016C-							
1H-1, 0-3	0.00	2.08	2.08	0.03	0.24	0.29	7.25
1H-1, 3-6	0.03	2.04	2.04	0.07	0.62	0.27	7.47
1H-1, 6-9	0.06	2.19	2.19	0.04	0.33	0.28	7.84
1H-1, 9-12	0.09	2.34	2.34	0.06	0.50	0.30	7.81
1H-1, 12-15	0.12	2.07	2.07	0.13	1.09	0.26	7.85
1H-1, 15-18	0.15	1.76	1.76	0.13	1.11	0.24	7.30
1H-1, 18-21	0.18	1.65	1.65	0.14	1.17	0.23	7.17
1H-1, 21-24	0.21	1.66	1.66	0.13	1.11	0.23	7.23
1H-1, 24-27	0.24	1.56	1.56	0.20	1.70	0.22	7.09
1H-1, 27-30	0.27	1.49	1.49	0.23	1.90	0.21	7.26

Note: TC = Total carbon, TOC = total organic carbon, IC = inorganic carbon, TN = total nitrogen, and $CaCO_3$ = calcium carbonate.

This is a sample of the table that appears on the volume CD-ROM.

Appendix C. Concentrations, odd/even carbon preference index, C_{31}/C_{27} ratio of long-chain *n*-alkanes, and estimated terrestrial and marine organic carbon contents of Core 167-1016C-1H sediments.

Core, section, interval (cm)	Depth (mbsf)	LNA (mg/g)	CPI	*n*-Alkane C_{31}/C_{27}	TROC (%)	MROC (%)
167-1016C-						
1H-1, 0-3	0.00	1.235	5.07	1.61	0.45	1.64
1H-1, 9-12	0.09	1.177	5.89	1.60	0.42	1.92
1H-1, 18-21	0.18	1.098	5.53	1.47	0.40	1.26
1H-1, 27-30	0.27	1.039	4.69	1.41	0.38	1.11
1H-1, 36-39	0.36	1.131	4.85	1.43	0.41	1.02
1H-1, 45-48	0.45	1.087	3.67	1.87	0.39	1.10
1H-1, 54-57	0.54	0.944	3.53	1.74	0.34	1.10
1H-1, 63-66	0.63	1.165	3.57	1.45	0.42	0.98
1H-1, 72-75	0.72	1.237	3.81	1.69	0.45	0.96
1H-1, 81-84	0.81	1.406	3.59	1.58	0.51	1.10

Note: LNA = long-chain *n*-alkanes, TROC = terrestrial organic matter, and MROC = marine organic matter.

This is a sample of the table that appears on the volume CD-ROM.

Appendix D. Concentrations of diatom- and prokaryote-derived compounds in Core 167-1016C-1H sediments.

Core, section, interval (cm)	Depth (mbsf)	$C_{25:4}$ HBIA (µg/g)	$C_{25:1}$ HBIA (µg/g)	Diploptene (µg/g)	Neohop-13(18)-ene (µg/g)	Fern-7-ene (µg/g)
167-1016C-						
1H-1, 0-3	0.00	0.232	0.036	0.183	0.042	0.072
1H-1, 9-12	0.09	0.496	0.036	0.216	0.046	0.091
1H-1, 18-21	0.18	0.232	0.030	0.118	0.034	0.064
1H-1, 27-30	0.27	0.129	0.019	0.096	0.025	0.053
1H-1, 36-39	0.36	0.136	0.030	0.100	0.028	0.056
1H-1, 45-48	0.45	0.017	0.032	0.157	0.042	0.102
1H-1, 54-57	0.54	0.013	0.038	0.097	0.031	0.072
1H-1, 63-66	0.63	0.000	0.042	0.106	0.039	0.078
1H-1, 72-75	0.72	0.000	0.051	0.113	0.037	0.085
1H-1, 81-84	0.81	0.000	0.053	0.136	0.057	0.117

Note: HBIA = highly branched isoprenoid alkene.

This is a sample of the table that appears on the volume CD-ROM.

Appendix E. Concentrations of petroleum-type compounds in Core 167-1016C-1H sediments.

Core, section, interval (cm)	Depth (mbsf)	DNH (µg/g)	αβS-Homohopane (µg/g)	αβR-Homohopane (µg/g)	ββ-Homohopane (µg/g)
167-1016C-					
1H-1, 0-3	0.00	0.092	0.032	0.027	0.054
1H-1, 9-12	0.09	0.095	0.025	0.025	0.069
1H-1, 18-21	0.18	0.099	0.025	0.021	0.043
1H-1, 27-30	0.27	0.082	0.024	0.019	0.036
1H-1, 36-39	0.36	0.084	0.024	0.020	0.041
1H-1, 45-48	0.45	0.074	0.033	0.044	0.055
1H-1, 54-57	0.54	0.070	0.024	0.032	0.046
1H-1, 63-66	0.63	0.099	0.032	0.043	0.060
1H-1, 72-75	0.72	0.105	0.035	0.044	0.066
1H-1, 81-84	0.81	0.137	0.045	0.043	0.071

Note: DNH = 17α(H),21β(H)-28,30-dinorhopane.

This is a sample of the table that appears on the volume CD-ROM.